

## EFFECT AND MEASUREMENT OF THE MACHINE COMPLIANCE IN THE MACRO RANGE OF INSTRUMENTED INDENTATION TEST

*Christian Ullner<sup>1</sup>, Erhard Reimann<sup>2</sup>*

<sup>1</sup> Federal Institute for Materials Research and Testing (BAM), Berlin, Germany, christian.ullner@bam.de  
<sup>2</sup> Zwick GmbH & Co., Ulm, Germany, erhard.reimann@zwick.com

**Abstract:** The contribution concerns the dominant source of uncertainty in the upper macro range of the instrumented indentation test. The strong effect of the machine compliance is demonstrated (including for machines with a displacement measurement which is related to the surface of the specimen). Four methods are applied for analyzing the experimental results up to 2500 N. The results show that the uncertainty of the compliance should be limited in ISO 14577 part 3 [1].

**Keywords:** indentation, compliance, uncertainty.

### 1. INTRODUCTION

The calibration of reference specimens according to ISO 14577 part 3 [1] needs not only the appropriate material but also a calibration machine of the required capability and the uncertainty of the delivered calibration values. A study on the estimation of uncertainty in instrumented indentation test [2] has shown that the machine compliance is an essential source of the uncertainty in the macro range. While the determination of the machine compliance in the nano and micro range is connected to the determination of the indenter area function [3-6] the machine compliance must be measured highly precise in the macro range. The present contribution reports on experiences concerning the measurement of the machine compliance.

### 2. CLASSIFICATION OF THE EFFECT

Let us consider the determination of the Martens hardness  $HM$  of silicone nitride using a machine with the compliance  $C_m$ . Because of the compliance of the machine, the measured depth  $h_{measured}$  at the test force  $F$  is the sum of the indentation depth  $h$  according to the definition of the Martens hardness [1] and the deformation of the machine

$$h_{measured} = h + C_m F = \sqrt{\frac{F}{G * HM}} + C_m F \quad (1)$$

with the geometric factor for the Vickers pyramid  $G=26.43$ .

The relative error of the measured indentation depth caused by the machine compliance reads

$$\frac{h_{measured} - h}{h} = C_m \sqrt{G * HM * F} \quad (2)$$

The results of (2) are plotted in Fig. 1 for three values of the machine compliance in  $C_m$ . Testing machines of the nano and micro range are mostly designed in such a way that the deformation of the machine frame is involved in the measurement of the indentation depth. The compliance of the frame is  $0.1 \mu\text{m/N}$  at least. Certain designs of machines in the macro range (depth measurement directly related to the surface of the specimen, see caption 4) lead to the machine compliance of about  $0.01 \mu\text{m/N}$ . As it will be shown in this paper, the determination of the machine compliance cannot be performed better than about  $0.001 \mu\text{m/N}$ .

Assuming an error of 1% can be accepted for the measurement of the indentation depth, three ranges are indicated by Fig. 1. While the correction is not needed up to about 25 mN, the indentation depth must be also corrected for the better designed machines if the test force exceed 2.5 N. The uncertainty of the measured compliance must be smaller than  $0.001 \mu\text{m/N}$  for of reliable indentation tests above 250 N. It should be noted, Fig. 1 gives only a finger print because the limits are dependent on the hardness of the specimen and the geometry of the indenter.

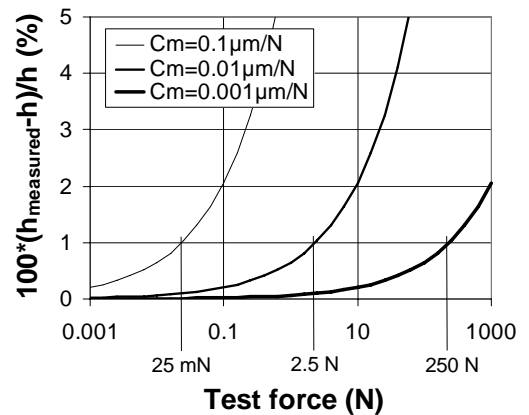


**Fig. 1. Relative deviation from the true indentation depth  $h$  as a function of the test force for silicon nitride ( $HM_{10/20} = 12000 \text{ N mm}^{-2}$ ) with Vickers pyramid. Typical compliances of nano indenter ( $0.1 \mu\text{m/N}$ ) and macro indenter ( $0.01 \mu\text{m/N}$ ) as well as the expected uncertainty of the compliance ( $0.001 \mu\text{m/N}$ ) are used.**

### 3. METHODS FOR DETERMINATION

According to ISO 14577 the indenter area function must be known for the determination of the machine compliance. Therefore, iterative methods are required in the nano and micro range [6]. Because the indentation depth is greater than 6  $\mu\text{m}$  for most cases in the macro range the compliance can be determined without the knowledge of the indenter area function. Besides, indentation modulus and hardness can be assumed to be independent of the test force.

#### 3.1. Constant indentation modulus (Method 1)

Indentation tests are performed at different forces  $F$ . The determined initial unloading slopes  $S(F)$  yield a set of indentation modulus  $E_{IT}(F)$ . Taking into account the measured total compliance  $C_t=1/S$  is the sum of the machine compliance and the real value  $C_{\text{real}}$  for the calculation of  $E_{IT}$ , the machine compliance  $C_m$  can be determined by variation of  $C_m$  and using a criteria for approaching  $E_{IT}(F)=\text{constant}$  (for instance, criteria of Gauss or vanish slope of the regression  $E_{IT}(F)$ ). It should be noted that the determination of the initial unloading slope can be done in different ways (linear regression within the selected range or nonlinear curve fitting and calculation of the derivate at  $F_{\text{max}}$ ).

#### 3.2. Linear regression in the plot $C_t$ vs. $F^{0.5}$ (Method 2)

The frequently used method is based on the definitions of indentation modulus  $E_{IT}$  and indentation hardness  $H_{IT}$  [1].

$$E_{IT} = (1 - \nu_s^2) \left( \frac{1}{E_r} - \frac{(1 - \nu_i^2)}{E_i} \right)^{-1} \quad (3)$$

$$\text{with } E_r = \frac{\sqrt{\pi} \left( \frac{dF}{dh} \right)_{F_{\text{max}}}}{2\sqrt{A_p}(h_c)} \quad (4)$$

$$H_{IT} = \frac{F}{A_p(h_c)} \quad (5)$$

Combining (4) and (5) with the total compliance,  $C_t=C_{\text{real}}+C_m$ , we obtain

$$\left( \frac{dh}{dF} \right)_{F_{\text{max}}} = C_m + \frac{\sqrt{\pi}}{2E_r} \frac{1}{\sqrt{A_p}(h_c)} = C_m + \frac{\sqrt{\pi}}{2E_r} \frac{\sqrt{H_{IT}}}{\sqrt{F}} \quad (6)$$

Again, indentation tests are performed at different  $F$ . The linear regression of the total compliance  $C_t$  against  $F^{0.5}$

$$\left( \frac{dh}{dF} \right)_{F_{\text{max}}} = C_t = C_m + \frac{\sqrt{\pi H_{IT}}}{2E_r} F^{-0.5} \quad (7)$$

gives the requested machine compliance  $C_m$  at infinite high force ( $F^{0.5} \rightarrow \infty$ ).

The method needs the assumptions of  $H_{IT}/E_r^2=\text{constant}$  and  $C_m=\text{constant}$  and the used extrapolation function must be correct. However, it should be noted the assumptions are fulfilled in practice if the plot  $C_t$  vs.  $F^{0.5}$  can be fitted by a straight line. It can be expected that the condition  $H_{IT}/E_r^2=\text{constant}$  is fulfilled better at higher forces in the extrapolation region.

Because (4) is independent of the indenter geometry [7] the determination of the machine compliance according to (7) is also possible for spherical indenters if the hardness is also defined by the quotient of force and contact area.

#### 3.3. Constant Martens hardness (Methods 3 and 4)

The rule of geometric similarity leads to a straight line in the plot square root of force  $F^{0.5}$  against indentation depth  $h$ . Therefore the Martens hardness  $HM_s$  should be constant. However, the curve deviates from the straight line if the machine compliance does not equal zero. For this reason, a set of  $HM_s^*(F)$  must be calculated from the measured indentation curve at different ranges of the force  $F$ .

For demonstrating the relationship between the  $HM_s^*$  calculated from the measured indentation curve and the  $HM_s$  corrected by the machine compliance  $C_m$  we start with the definition of the measured  $HM_s$

$$HM_s = \frac{1}{G} \left( \frac{d\sqrt{F}}{dh} \right)^2 \quad (7)$$

After re-arranging of (7) and integrating by  $F^{1/2}$  we get

$$h_{\text{measured}} = h_0 + \sqrt{\frac{F}{G * HM_s^*}} \quad (8)$$

with the integration constant  $h_0$ . Now the correction of the machine compliance can be done.

$$h = h_0 + \sqrt{\frac{F}{G * HM_s^*} - C_m F} \quad (9)$$

After the differentiation by  $F^{1/2}$  and re-arranging, (9) and (7) give the requested  $HM_s$  corrected by the machine compliance  $C_m$ .

$$HM_s = HM_s^* \left( 1 - 2C_m \sqrt{HM_s^* \cdot G \cdot F} \right)^{-2} \quad (10)$$

The machine compliance can be determined by variation of  $C_m$  and using a criteria for approaching  $HM_s(F)=\text{constant}$  (for instance, criteria of Gauss or vanish slope of the regression  $HM_s(F)$ , method 3).

However, a more detailed insight is given by fitting the inverse function  $h_{\text{measured}}$  against  $F^{0.5}$  using the following equation which is demonstrated by the analogous steps as done from (7) to (9).

$$h_{\text{measured}} = h_0 + \sqrt{\frac{F}{G * HM_s^*} + C_m F} \quad (11)$$

The coefficients of the polynomial of second order for  $F^{0.5}$  give the correct zero point  $h_0$ , the Martens hardness  $HM_s$ , and the machine compliance  $C_m$  (method 4). The same equation is recommended to use in [3] for estimating the indenter tip radius from the parameter  $h_0$ . Plotting  $(h-h_0)F^{0.5}$  against  $F^{0.5}$  the slope of the curve is the wanted machine compliance. Deviations of the straight line in such a plot should indicate the force dependence of the machine compliance.

## 4. EXPERIMENTAL

The experiments were performed at BAM and Zwick GmbH & Co. using different testing machines (Zwick Z005 and Zwicky) which were equipped with different hardness measuring heads ( $F_{\max} = 200 \text{ N}$  and  $F_{\max} = 2500 \text{ N}$ ) and different Vickers indenters (including combinations). The force resolution is about  $0.01 \text{ N}$  and  $0.1 \text{ N}$ , respectively. Both heads have an incremental displacement measurement system based on a glass scale with a resolution of  $20 \text{ nm}$  or  $40 \text{ nm}$ . The arrangement of the displacement measurement is shown in Fig. 2. The displacement is measured directly between the surface of the specimen and a place above the indenter. Therefore the measured displacement is independent of deformation within the loaded machine frame. However, even the loaded element between the place of the glass scale and the indenter tip gives a small contribution to the measured displacement because its compliance is about  $0.01 \mu\text{m/N}$  (Fig. 1).

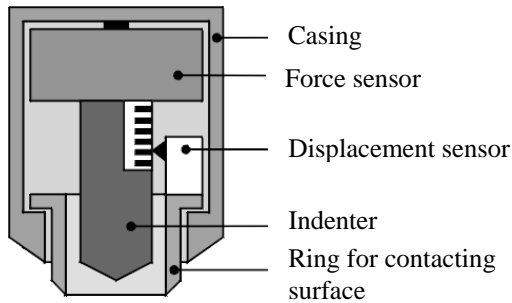


Fig. 2. Sketch of the Zwick hardness head.

The tests were conducted in two groups. Common stainless steel (X8CrMnN18-18) and two hardness blocks (2044HV3, 128HV1) were used for comparison of the methods described in caption 3. The indentations were done with the same Vickers indenter using the machine Z005 equipped with the 200N-hardness head. The test force was applied with about  $8 \text{ N/s}$  up to  $18.5 \text{ N}$ ,  $47 \text{ N}$ ,  $89 \text{ N}$ ,  $141 \text{ N}$ , and  $200 \text{ N}$  in two modes. One series of 10 indentations is done at the same position on the specimen and the other series is done at different indentation positions. The holding periods at the five maximum forces were  $60 \text{ s}$ . Because the force removal rate is about  $8 \text{ N/s}$  and the creep rate at the end of the holding period is smaller than  $3 \text{ nm/s}$ , the determined initial unloading slope  $S < 60 \text{ N}/\mu\text{m}$  may not be influenced by the continued creep. To determine the initial unloading slope precisely enough the data are stored after every depth variation of  $20 \text{ nm}$ .

The second group of the tests concerns the question if different indenters in different machines results to different values of the machine compliance. Indentations were done with force application rates and force removal rates of  $100 \text{ N/S}$  ( $10 \text{ N/s}$ ) up to  $2500 \text{ N}$  ( $200 \text{ N}$ ) on hardness blocks 772HV ( $26.5\text{HRC}$ ) and float glass using two machines of the type Zwicky. The holding periods were  $20 \text{ s}$  ( $120 \text{ s}$ ). Only one force cycle was conducted and the results were analyzed by calculating the parameters of (11).

## 5. RESULTS AND DISCUSSION

### 5.1 Comparison of the methods

Using different methods the machine compliance has been calculated from identical data files. Selected results are collected in Table 1. As expected the values are very small because the indentation depth is measured in relation to the surface of the specimen. In fact, the indenter holder is a cylinder made of steel ( $E = 208 \text{ GPa}$ ) with a diameter  $d = 6.35 \text{ mm}$  which gives a calculated compliance of  $4.5 \text{ nm/N}$  if the distance between indenter tip and displacement sensor is about  $30 \text{ mm}$  (Fig. 2). However, the machine compliance determined by the four methods can be influenced additionally by tilting or deforming the specimen. Because the surface is contacted by the ring outside of the indenter (Fig. 2) and the displacement is not measured within the loading axis of the indenter (Abbe's rule is not fulfilled), any movement of the specimen can disturb the depth measurement.

Table 1. Results of the machine compliance  $C_m$  in  $\text{nm/N}$  for the same data files of Vickers indentations

	Method 1	Method 2	Method 3	Method 4
Material	Constant $E_{IT}$	Constant $H_{IT}/E_r^2$	Constant $HM_s$	Fit of (11)
2044HV3	5.3	4.5	6.8	7.4
128HV1	5.2	4.2	6.5	5.5
X8CrMnN 18-18	3.4	3.9	6.1	-

Considering the estimated uncertainty of the materials parameter [2] or the demonstration in Fig. 1, the differences between the values collected in Table 1 are not sufficiently small for the macro range. Using method 1 the determination of the initial unloading slopes  $S$  are included. The values in Table 1 are based on the determination of  $S$  by a linear fit. The non-linear fit which is also accepted by the standard [1] leads to values which can deviate from those of Table 1 by about  $1 \text{ nm}$ . Similar deviations occur if averages are used instead of the individual values and if the minimum of the residual square sum is used instead of the vanish slope in the linear regression of  $E_{IT}(F)$ . It should be noted, that the use of Young's modulus  $E = 208 \text{ GPa} = E_{IT}$  for the determination of the machine compliance does not result to  $E_{IT}(F) = \text{const}$ . The reason seems to be the pile-up effect on steel. The values in Table 1 lead to  $E_{IT}$  and  $HM_s$  collected in Table 2.

Fig. 3 demonstrates the good results of method 2. As expected the absolute term of the linear regression (equals to the machine compliance) is the same for the three materials with different numbers of hardness and Young's modulus. Only the slope of the straight lines is different according to (7). The resulting compliances are smaller by about  $1 \text{ nm}$  than the results obtained by method 1. The small difference could be caused by the use of averages instead of individual values.

Different results are also observed in Table 1 if different ways are used in method 3. The Martens hardness  $HM_s$  has been calculated within the range of  $0.5F_{\max} < F < 0.98F_{\max}$ . As done for method 1 the machine compliance is

determined by searching the slope 0 in the linear regression of the individual values of  $HM_s(F)$ . An additional deviation could arise if the depth dependence of the hardness is not exactly quadratic [8]. However, the effect of time dependent hardness is so poor that it cannot be separated from the effect of machine compliance.

**Table 2. Averages (left) and standard deviations (right) of the materials parameters calculated from the same data files on the base of the machine compliances collected in Table 1.**

	Method 1	Method 2	Method 3	Method 4
	Constant $E_{IT}$	Constant $H_{IT}/E_r^2$	Constant $HM_s$	Fit of (11)
<b>2044HV</b>				
$E_{IT}$ (GPa)	691 32	655 37	747 30	
$HM_s$ (Nmm <sup>-2</sup> )	16690 320	16310 350	17240 390	17130 540
$h_0$ (μm)				24 29
<b>128HV</b>				
$E_{IT}$ (GPa)	240 25	226 23	263 29	
$HM_s$ (Nmm <sup>-2</sup> )	1410 20	1400 21	1420 20	1400 30
$h_0$ (μm)				-107 96

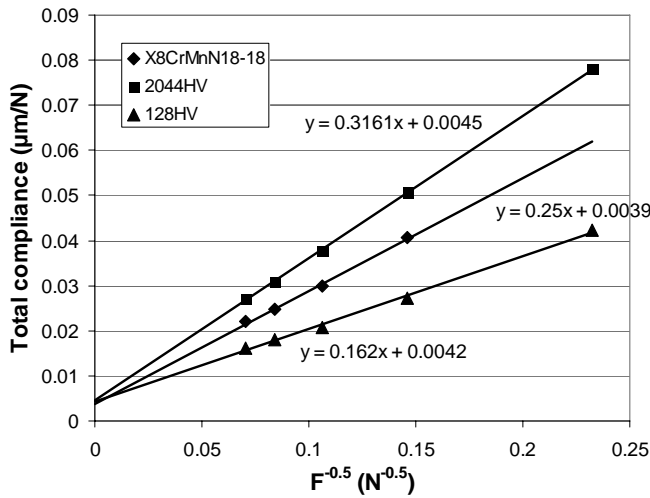


**Fig. 3. Determination of the machine compliance  $C_m$  by extrapolation to  $F^{0.5}=0$  (method 2).**

Assuming the force independence of the hardness is valid the simplest and most effective way to determine compliance and hardness is the method 4. While the resulting hardness (Table 2) agrees well with the hardness determined by method 3 the compliance differs by some nm/N (Table 1). Again, it must be checked if the difference could be caused by the existing force dependence. In fact, it can be shown by a simple simulation that the Meyer exponent of 1.8 (instead of 2) in the plot  $\log F$  vs.  $\log h$  leads to a virtual machine compliance of less than 1 nm/N by using the plot  $h$  vs.  $F^{0.5}$  according to (11). Therefore, the resulting compliance determined by method 4 can be influenced poorly by the force dependence.

Let us use (11) to check if the machine compliance is really independent of the force, as assumed. The parameter  $h_0$  in Table 2 is very small related to the depth  $h$  and can be neglected from depths greater than about one μm. It can be concluded from (11) that the slope of the plot  $h/F^{0.5}$  vs.  $F^{0.5}$  is the compliance. Fig. 4 presents the indentation data of 2044HV3 used for calculating the numbers in the Tables 1 and 2. Obviously, the compliance is only constant for forces greater than about 36 N. The fluctuations seem to be similar for all indentations. Likely, the fluctuations indicate the certain feature of the displacement measuring system in connection with the small movement of the specimen under load. In the region of constant slope,  $F > 36$  N, the compliance varies from 5.5 nm/N to 7.9 nm/N but in the force range  $2 \text{ N} < F < 16 \text{ N}$  the slope increases up to 15 nm/N. It should be checked in future if the indicated force dependence is really based on nonlinear machine compliance or is caused by uncertainties in the force and displacement measurement. The strong fluctuations for  $F < 4 \text{ N}$  occur because of the surface roughness and layers due to preparation and aging. Therefore the parameter  $h_0$  in (11) and Table 2 is not appropriate to determine the tip radius of the indenter as it is recommended in [3].

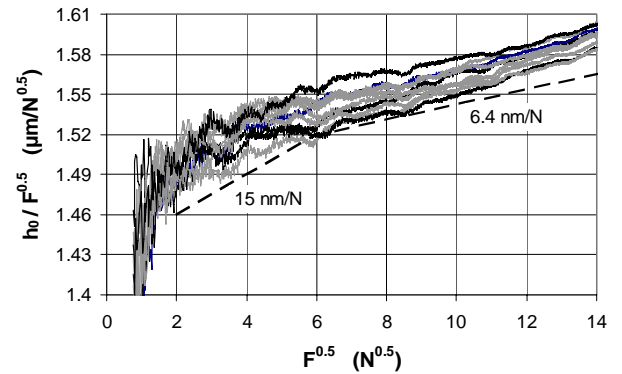


**Fig. 4. Demonstration of the check if the machine compliance  $C_m$  is independent of the test force. The slope of the curve is the machine compliance.**

## 5.2 Comparison of different indenters and machines

The results of the instrumented indentation tests performed on two hardness blocks and float glass are collected in Table 3. In addition to the comparison of different machines and indenters the feature of method 4 should be studied in more detail. Therefore, different ranges of the indentation curves are used for the determination of the compliance and the results are compared with the compliance  $C_{208}$  which is calculated from the initial unloading slope  $S$  according to (6) and using the reference value of the Young's modulus,  $E = 208 \text{ GPa}$ .

As expected the holding period does not affect the results (T1-T2 and T5-T6 in Table 3) because the compliance is calculated from the increasing part of the indentation curve up to  $F_{max}$ . However, the missing effect can also be shown by the compliance  $C_{208}$ . The numbers of  $C_{208}$  also show that the influence of the machine (T2-T4 and T6-T8) seems to be lower than the influence of the Vickers

indenter (T2-T3, T6-T7) but the scatter of the numbers determined by method 4 does not allow to get a reliable result .

The results which are obtained by using the largest range, 6  $\mu\text{m}$  to 2500 N, are very precise (Table 3). Especially the repeatability of about 0.2 nm/N shows that the uncertainty of the compliance can be roughly estimated by about 1 nm/N for testing laboratories. To achieve an uncertainty of less than 0.5 nm/N for calibration machines an all-embracing new design is needed [9]. To demonstrate the potential check of the precision Fig. 5 shows the individual data files of the reference block 772HV0.1 (T7) in the plot

$$\frac{(h_{\text{measured}} - h_0)}{\sqrt{F}} - \sqrt{\frac{1}{G^* HM_s}} \text{ vs. } \sqrt{F} \quad (12)$$

according to (11) after re-arranging.

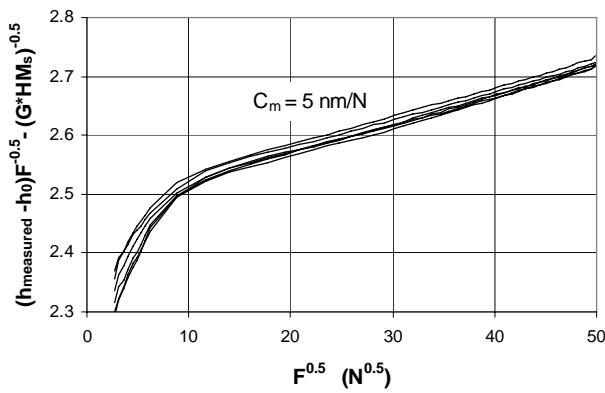


Fig. 5. Demonstration of constant compliance in the force range of 200 N < F < 2500 N by plotting the data according to (12).

If the range of analyzing is limited to 200 N the averages of the compliances are significantly higher (Table 3 and Fig. 5). The higher compliance at smaller forces has been already found for another Vickers indenter (Fig. 4). The force dependend compliance at smaller forces could be caused by the certain compound between the diamond pyramide and the indenter-holder. The effect can be detected only by the very sensitive method 4.

However, method 4 is based on the assumption that the hardness  $HM_s$  is constant. The assumption could not be fulfilled by a certain feature of the material. For instance, cracking is generated in glass by indentation. Although the indentation curves of glass (T9 in Table 3) are very smooth the compliance determined by method 4 is higher than the results which are obtained by using the metallic reference blocks. It should be noted, that the standard deviations in the case of glass are small although the force is 200 N (Table 3) and initial cracking is observed above 6 N. Therefore, common float glass with the very good surface quality could be used in connection to method 4 as an appropriate tool for checking the property of the indenter for the application in the macro range.

## 6. CONCLUSION

Because the machine compliance has an important influence on the parameters of the instrumented indentation test in the macro range four methods have been used to calculate the compliance. For the used indenter and machines, the resulting numbers are very small (3.5 nm/N to 15 nm/N). Differences could be caused by the specified materials behavior and by the force dependence of the compliance. While the method 2 gives the most reliable values the method 4 is well appropriate to detect the force dependence. Regarding the uncertainty in determining the compliance of about 1 nm/N any differences between different machines and indenters could not be detected reliable. The compliance is 10-15 nm/N in the force range up to 36 N and decreases to the constant value of about 4 nm/N in the force range from 100 N to 2500 N.

Obviously, requirements for the determination of compliance should be involved in the ISO 14577 part 3 concerning the used method and range. A maximum permissible uncertainty of the compliance should be given for the reference machine. If the uncertainty of the machine compliance cannot be reduced to less than 1 nm/N the macro range should be limited to the maximum force of 2500 N in ISO 14577 part 1.

Table 3. Compliance of different machines (M) with different Vickers indenters (I). Indentation tests (indicated by T) were performed n-times up to  $F_{\text{max}}$ . The holding period was  $\Delta t$ . The machine compliance was determined by method 4 within different ranges of the indentation curves. The compliance  $C_{208}$  was calculated from the initial unloading slope S according to (6) and using the reference value of the Young's modulus 208 GPa.

T	Material	M	I	n	$F_{\text{max}}$ N	$\Delta t$ s	Machine Compliance $C_m$ (nm/N)								S N/ $\mu\text{m}$	$C_{208}$ nm/N		
							6 $\mu\text{m}$ - 2500N		2 $\mu\text{m}$ - 200N		200N - 2500N		2 $\mu\text{m}$ - 36N				36N - 200N	
1	26,5HRC	1	1	7	2500	120	4.4	0.2	6.2	2.9							125.1	2.7
2	26,5HRC	1	1	7	2500	20	4.7	0.2	7.1	2.2	4.7	0.3	13.2	8.2	8.7	5.0	123.8	2.8
3	26,5HRC	1	2	8	2500	20	5.4	0.9	9.8	3.4	5.4	0.9	24.0	8.2	-6.6	9.8	116.0	3.3
4	26,5HRC	2	1	5	2500	20	5.2	0.3	6.1	1.1							123.1	2.8
5	772HV	1	1	7	2500	120	3.5	0.3	8.4	0.9							89.4	2.7
6	772HV	1	1	6	2500	20	3.5	0.2	9.0	1.3	3.4	0.1	8.8	3.5	3.9	1.4	89.4	2.6
7	772HV	1	2	6	2500	20	5.0	0.1	6.4	1.1	5.4	0.1	19.7	4.1	-0.3	1.1	86.4	3.0
8	772HV	2	1	7	2500	20	4.6	0.2	7.4	0.6	4.6	0.3	9.0	4.2	4.9	1.6	87.2	2.9
9	Glass	1	1	6	200	20			10.2	1.9			15.9	2.5			12.3	9.6

## REFERENCES

- [1] ISO 14577: Metallic materials - Instrumented indentation test for hardness and other materials parameters; October 2003  
- part 1: Test method  
- part 2: Verification and calibration of the testing machine  
- part 3: Calibration of reference test pieces.
- [2] Ch. Ullner, "Critical points in ISO 14577 part 2 and 3 considering the uncertainty in measurement," Proc. of HARDMEKO 2004, 11-12 November, 2004, Washington D.C., USA
- [3] Y. Sun, S. Zheng, T. Bell, J.F. Smith, "Indenter tip radius and load frame compliance calibration using nanoindentation loading curves", *Philosophical Magazine Letters*, vol. 79, no. 9, pp. 649-658, 1999
- [4] K.J. Van Vliet, L. Prchlik, J.F. Smith, "Direct measurement of indentation frame compliance", *J. Mater. Res.*, vol. 191, pp. 325-331, 2004.
- [5] A.L.M. Costa, D.J. Shuman, R.R. Machado, M.S. Andrade, "Determination of the compliance of an instrumented indentation testing machine", *Proc. of HARDMEKO 2004*, 11-12 November, 2004, Washington D.C., USA
- [6] ISO DIS 14577: Metallic materials - Instrumented indentation test for hardness and other materials parameters - Part 4: Test method for metallic and non-metallic coatings; October 2005.
- [7] G.M. Pharr, W.C. Oliver, F.R. Brotzen: On the generality of the relationship among contact stiffness, contact area, and elastic modulus during indentation; *J. Mater. Res.* 7(1992), 613-617
- [8] P. Grau, G. Berg, H. Meinhard, S. Mosch, "Strain Rate Dependence of the Hardness of Glass and Meyer's Law", *J. am. Ceram. Soc.* vol. 81, pp. 1557-1564, 1998.
- [9] H. Kohlhoff, Ch. Ullner, "Design and capability of a new calibration machine for the macro range of instrumented indentation test", IMEKO XVIII World Congress 2006, TC 5